

Role of B'' Ion (B'' = Nb, Ta) on perovskite development, lattice parameters and dielectric properties of (Ba,Pb)(Zn_{1/3}B''_{2/3})O₃ ceramics

BYUNG-YONG AHN, NAM-KYOUNG KIM

Department of Inorganic Materials Engineering, Kyungpook National University, Taegu 702-701, Korea

E-mail: nkkim@knu.ac.kr

Ceramic powders of Pb(Zn_{1/3}B''_{2/3})O₃ (where B'' is Nb or Ta ions) complex-perovskite compositions, with gradual replacements of Pb by Ba, were prepared by using a B-site precursor method. Phases developed in both systems were identified by X-ray diffraction and perovskite contents were evaluated as a function of the amount of Ba substitution. Variations of lattice parameters of the pyrochlore and perovskite structures with composition modifications are interpreted in terms of the 6- and 12-fold cation sizes. Weak-field dielectric properties of the two systems in the low-frequency range are compared. © 2002 Kluwer Academic Publishers

1. Introduction

Lead zinc niobate Pb(Zn_{1/3}Nb_{2/3})O₃ (PZN) is one of the typical complex-perovskite ferroelectric relaxor compounds of Pb(B', B'')O₃-type, possessing high dielectric constant values and diffuse nature in the phase transition mode [1, 2]. Divalent and pentavalent cations of Zn and Nb in PZN are known to occupy the octahedral sublattices of the perovskite structure in a disorderly manner [1–4]. Perovskite PZN powders could only be synthesized under high pressures [5] or via mechanochemical routes [6], whereas single-crystalline forms were prepared by flux-growth methods [1–3, 7, 8]. By a simple replacement of Nb by Ta in PZN, a tantalum-analog perovskite stoichiometry of lead zinc tantalate Pb(Zn_{1/3}Ta_{2/3})O₃ (PZT) is expected to form. It should be noticed that PZT in the present paper does not stand for Pb(Zr,Ti)O₃. So far, however, any attempt to synthesize PZT has been unsuccessful and perovskite PZT still resists ready formation by any means [9–11]. Meanwhile, barium zinc niobate and tantalate of Ba(Zn_{1/3}Nb_{2/3})O₃ and Ba(Zn_{1/3}Ta_{2/3})O₃ (BZN and BZT, respectively) belong to an important microwave dielectric group of superior properties with low losses [12–15]. In contrast to the perovskite PZN and PZT, the barium-analogs of BZN and BZT readily assume the perovskite structure [16–18]. Besides, Zn and Nb ions in BZN [19, 20], and Zn and Ta in BZT [18, 21] as well, are reported to exhibit long-range structural ordering at the 6-fold sublattices of the perovskite structure.

The Goldschmidt tolerance factor (TF) values of PZN and PZT, and of BZN and BZT, are calculated to be the same, as ionic radii of Nb and Ta are reported to be identical, 0.064 nm [22]. When Pb (0.149 nm [22]) at the 12-fold lattice sites are replaced by larger

Ba (0.161 nm [22]), the values of the electronegativity difference (END) as well as TF would increase accordingly. Actually, additions of polar dielectric BZN and BZT to PZN and PZT, respectively, are reported to stabilize the perovskite structure quite substantially [23–25], as stability of the perovskite would be enhanced by the increased values of END and TF. On the other hand, END value of PZT is lower than that of PZN, indicating more-covalent nature in the former. Hence PZT is known to be more difficult to adopt an ionic crystal structure of perovskite.

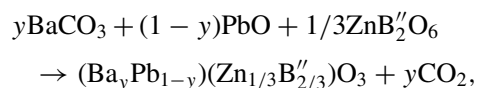
In the present study, results of Pb(Zn_{1/3}B''_{2/3})O₃ (where the B'' cation is pentavalent Nb or Ta), with gradual replacements of Pb by Ba, are compared with respect to the perovskite synthesis, lattice parameter changes, and dielectric properties. In order to suppress the pyrochlore formations and thereby to increase the perovskite phase yields, a two-stage reaction of B-site precursor method [26, 27] (more comprehensive terminology for the so-called columbite process [28] was used, where (Zn_{1/3}B''_{2/3})O₂ powders were prepared separately and were used as precursors for the perovskite syntheses.

2. Experimental

Two-stage reaction routes of the B-site precursor method are as follows;



and



where y ($=0.0, 0.2, 0.4, 0.6, 0.8,$ and 1.0) stands for the mole fractions of substituent Ba. Near the composition ranges of interest, the regular intervals of 0.2 were subdivided in order to closely explore the characteristics. It should be noted that although $(\text{Ba}_y\text{Pb}_{1-y})(\text{Zn}_{1/3}\text{Nb}_{2/3})\text{O}_3$ and $(\text{Ba}_y\text{Pb}_{1-y})(\text{Zn}_{1/3}\text{Ta}_{2/3})\text{O}_3$ (BPZN and BPZT systems, respectively) are written in the perovskite forms, they simply denote the nominal compositions and do not necessarily indicate formations of the perovskite structure in the entire composition ranges of $0.0 \leq y \leq 1.0$. All of the starting materials were oxides, except for BaCO_3 , with chemical purities of $>99.5\%$. Moisture contents of raw materials and synthesized $\text{ZnB}_2''\text{O}_6$ precursors were measured and introduced to the batch calculation in order to maintain the powder compositions as closely to the nominal values as possible.

Precursor powders of ZnNb_2O_6 and ZnTa_2O_6 (formed at 1150 and 1200°C , respectively) were reacted with BaCO_3 and PbO by stoichiometric proportions of $1:3$ molar ratios (i.e., without any addition of excess amount) at $900\text{--}1000^\circ\text{C}$ for 2 h, with intermediate milling/drying steps to promote phase formations. Developed structures after the calcinations were checked by powder X-ray diffraction (XRD). Lattice parameters of the pyrochlore and perovskite structures were calculated using the XRD data, assuming (pseudo)cubic symmetries. Perovskite phase yields were estimated by the usual method of simple comparison between major peak intensities of pyrochlore (222) and perovskite (110) reflections, i.e., $I_{\text{perov.}}/(I_{\text{pyro.}} + I_{\text{perov.}})$. Prepared powders were pressed isostatically into pellets and were densified for 1 h at $1000\text{--}1400$ and $1200\text{--}1450^\circ\text{C}$ for the BPZN and BPZT systems, respectively, in a multiple-crucible setup [29] in order to minimize lead loss during firing. Calcination and sintering temperatures of the BPZT system compositions were somewhat higher than those of the BPZN in general, because of the refractory nature of Ta_2O_5 . Sintered pellets were ground/polished and gold-sputtered on major faces as electrodes. Dielectric constant spectra were measured using an impedance analyzer at $1, 10, 100,$ and 1000 kHz (oscillation level $= 1 V_{\text{rms}}$).

3. Results and discussion

In Fig. 1 are XRD spectra of the calcined products from the Pb-Zn-Nb-O and Pb-Zn-Ta-O stoichiometric mixtures intended for perovskite development. The pyrochlore and perovskite patterns are taken from $\text{Pb}_{1.83}(\text{Zn}_{0.29}\text{Nb}_{1.71})\text{O}_{6.39}$ (JCPDS #34-374) and $\text{Pb}(\text{Zn}_{1/3}\text{Nb}_{2/3})\text{O}_3$ (JCPDS #22-662), while those of PbO and ZnO are from JCPDS #38-1477 and #36-1451, respectively. Since XRD spectrum of the pyrochlore (in Fig. 1) is virtually identical to that of $\text{Pb}_{1.83}(\text{Zn}_{0.29}\text{Ta}_{1.71})\text{O}_{6.39}$ (JCPDS #36-1451), except for minor mismatches in intensity (due to different scattering factors between Nb and Ta), the latter pattern is not shown. Similarly XRD pattern of perovskite-structured $\text{Pb}(\text{Zn}_{1/3}\text{Ta}_{2/3})\text{O}_3$ is not included either, as corresponding data are not available. However, by an analogy between the pyrochlore compounds of $\text{Pb}_{1.83}(\text{Zn}_{0.29}\text{Nb}_{1.71})\text{O}_{6.39}$ and

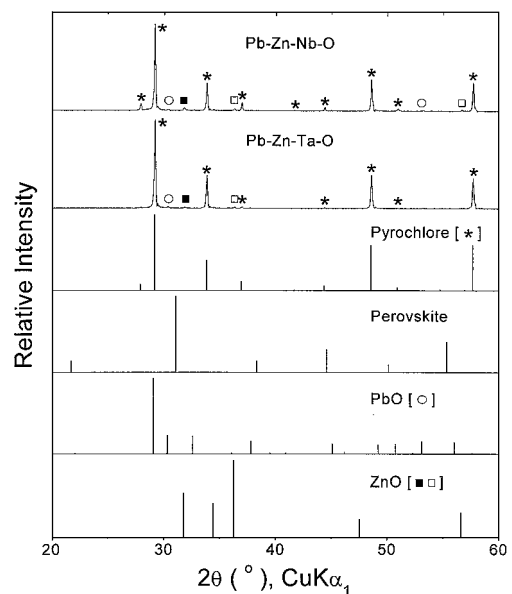


Figure 1 Phases developed from the Pb-Zn-Nb-O and Pb-Zn-Ta-O compositions ($y = 0.0$). Diffraction data of perovskite, pyrochlore, PbO , and ZnO are also shown for comparison.

$\text{Pb}_{1.83}(\text{Zn}_{0.29}\text{Ta}_{1.71})\text{O}_{6.39}$, and also by considering the identical ionic radii of Nb and Ta (0.064 nm [22]), X-ray pattern of the hypothetical perovskite PZT is expected to be close to that of the perovskite in Fig. 1.

Overall spectra of the two compositions of Pb-Zn-Nb/Ta-O are quite similar (except for minor differences in intensity), where pyrochlore was the dominant phase without any trace of the perovskite. Besides, all of the other extraneous peaks could satisfactorily be identified as those of PbO and ZnO , which are believed to be the by-products left after the pyrochlore formation from mixtures of perovskite stoichiometries. The strongest peak ($2\theta \simeq 29.1^\circ$) of PbO was undoubtedly obscured by the pyrochlore (222) reflection of the highest intensity located at $2\theta \simeq 29.2^\circ$. Even though perovskite developments (up to 5% and 2%) in the Pb-Zn-Nb/Ta-O compositions were claimed by Ling *et al.* [30], all of the reflections (except for those of PbO and ZnO) in Fig. 1 matched to those of the pyrochlore. By comparing the perovskite contents in Table I [30] and diffraction data in Table III [31], the perovskite content of 5% (after 800°C calcination) seems to be the calculation result of $5.1/(100.0 + 5.1)$, where 5.1 (line #4) is the relative intensity of the 31.73° peak. A small reflection was also detected at the same position in the present study (marked by ■), but the peak could rather be interpreted to belong to ZnO and not to perovskite. Presence of ZnO was also supported by other reflections (marked by □), too. Besides, as their method was a conventional one-step solid-state reaction (which is undoubtedly less efficient in the preparation of complex perovskite compositions [26-28]), it is cautiously speculated that they might have misinterpreted the 31.73° peak to be the perovskite (110) reflection of the highest intensity.

Perovskite formation yields in the two systems were estimated from the atmosphere powders (used during the sintering process) and the results are compared in Fig. 2. In both of the BPZN and BPZT systems, the yield increased asymptotically to 100% with increasing Ba

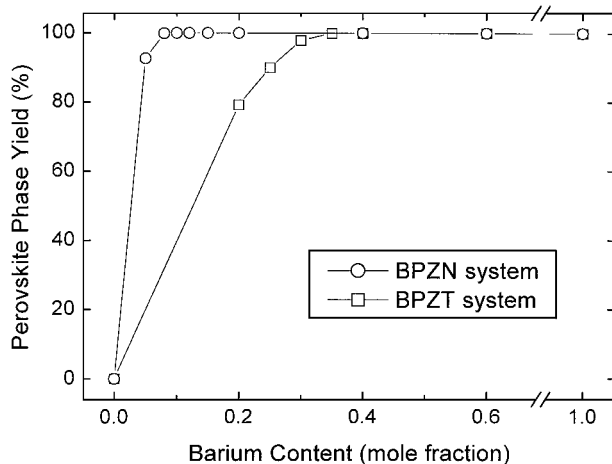


Figure 2 Perovskite contents of the BPZN and BPZT system compositions.

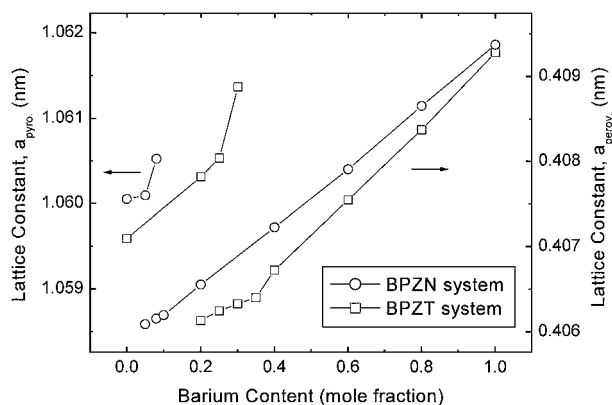


Figure 3 Variations of the lattice parameters of the pyrochlore and perovskite structures.

substitution. The perovskite structure in PZN, however, was fully stabilized at a much smaller barium concentration of ≥ 8 at.% than ≥ 35 at.% in PZT. Consequently the slope in the pyrochlore-perovskite diphasic composition range was much steeper in the former system. The rather sluggish increase in the BPZT system can be accounted for by the stronger covalency of PZT, which is evident from the smaller END value of $X_{\text{Ta-O}}$, as compared with that of $X_{\text{Nb-O}}$ [32].

Lattice parameter changes in the BPZN and BPZT systems are presented in Fig. 3. Both parameters of the pyrochlore and perovskite structures are shown below the threshold barium concentrations, whereas only the perovskite values are plotted above the diphasic composition ranges. Fairly linear relationships in the perovskite parameters above the threshold concentrations in both systems indicate formations of perovskite solid solutions. It is interesting to note that overall perovskite parameters in the BPZN system were larger than those in BPZT, despite identical sizes of Nb and Ta [22]. Similar cases of larger parameters in the Nb-containing complex perovskite compounds (as compared with the tantalates) could also be found in the cases of $\text{Pb}[\text{Li}_{1/4}(\text{Nb}/\text{Ta})_{3/4}]\text{O}_3$ [33], $\text{Pb}[\text{Mg}_{1/3}(\text{Nb}/\text{Ta})_{2/3}]\text{O}_3$ [34], $\text{Pb}[\text{Fe}_{1/2}(\text{Nb}/\text{Ta})_{1/2}]\text{O}_3$ [35–37], $\text{Pb}[\text{Sc}_{1/2}(\text{Nb}/\text{Ta})_{1/2}]\text{O}_3$ (JCPDS #43–134, 43–135), etc. From such instances, it is likely to conclude that ionic size of Ta is actually somewhat smaller than

that of Nb (at least in the lead-based complex perovskite structure), in contrary to the identical values reported [22].

Lattice parameters of BZN and BZT were calculated to be 0.4094 and 0.4093 nm, which are almost identical to the reported value of 0.40935 nm (JCPDS #39–1474) and 0.4092 nm (JCPDS #29–203), respectively. For ready comparison, hexagonal lattice parameters of BZT were converted to a cubic one by taking a cube root of the unit cell volume. Meanwhile, lattice parameter of perovskite PZN (as extrapolated from the linear region above the threshold concentration) is 0.4058 nm, which is close to a reported value of 0.4062 nm (JCPDS #22–662). On the other hand, similarly-obtained parameter of hypothetical perovskite PZT, 0.4050 nm, cannot be compared with any value at the moment due to unavailability. The estimation can, however, be still used as a prediction, if ever perovskite PZT be synthesized by whatever means. Lattice parameters of the pyrochlore structure developed in the Pb-Zn-Nb-O and Pb-Zn-Ta-O compositions (i.e., $y = 0.0$) were 1.0600 and 1.0596 nm, respectively, which are also close to the reported values of 1.06017 nm (JCPDS #34–374) and 1.05983 nm (JCPDS #34–395). The parameter of the Ta-containing pyrochlore is also smaller than that of the niobate, as in the parameters of the perovskite systems.

Moreover, increasing rate of perovskite lattice parameters of 3.52 pm/Ba fraction ($0.1 \leq y \leq 1.0$) in the BPZN system is somewhat smaller than 4.25 pm/Ba fraction in BPZT ($0.4 \leq y \leq 1.0$). Hence, difference in the parameter of up to 0.5 pm between the two systems at $y = 0.4$ decreased to 0.1 pm at $y = 1.0$, in spite of the same changing rates in the tolerance factors in both systems. Similar instances of smaller difference in the perovskite lattice parameters, when pentavalent B'' cations are either Nb or Ta, are also found in $(\text{Pb}/\text{Ba})(\text{Sc}_{1/2}\text{B}'_{1/2})\text{O}_3$ (JCPDS #43–135, #43–134, #24–1032, #19–134), whose parameters lead to 3.9 and 4.3 pm/Ba fraction for the niobate and tantalate compounds, respectively. The two slopes are comparable to the values obtained in the BPZN and BPZT systems, even though fractions of Nb (or Ta) in the octahedral components are somewhat different: 1/2 vs. 2/3, i.e., 3 : 4. Such decreases in the difference of the lattice parameters with increasing A-site cation sizes can be explained by considering relative sizes of the 6- and 12-fold ions. Influence of the size difference in the B-site octahedral lattice to the unit cell dimension is comparatively greater when A-site components are smaller, i.e., at Ba-poor compositions or low values of y in the present study. In contrast, the effect would be rather diluted in larger A-site cases of higher y or Ba-rich compositions.

The nearly-constant decreasing rates in the perovskite parameters with increasing lead concentrations in the monophasic perovskite ranges suddenly became considerably smaller at Pb-rich compositions near the threshold barium concentrations in both systems. The changes in the slope can possibly be explained by preferential consumption of Pb component in the pyrochlore formations, thus resulting in the coexisting perovskite phases of richer in Ba than

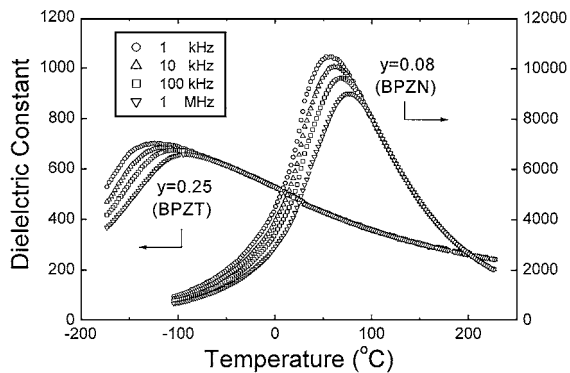


Figure 4 Frequency-dependent dielectric constant spectra of $y = 0.08$ (BPZN) and $y = 0.25$ (BPZT).

nominal compositions, which would lead to expansion of the unit cell. Meanwhile, lattice parameter ratios between the pyrochlore and perovskite structures ($a_{\text{pyro.}}/a_{\text{perov.}}$) in the two systems are nearly constant to be 2.610–2.612, which are in excellent agreement with those of earlier reports for $\text{Pb}(\text{B}', \text{Nb}/\text{Ta})\text{O}_3$ compounds [30, 31], regardless of the B' species. Similar to the cases of the perovskite, lattice parameters of the pyrochlore also showed definite bending points at compositions somewhat below the threshold concentrations.

Dielectric constant spectra of representative compositions $y = 0.08$ (BPZN) and $y = 0.25$ (BPZT) are contrasted in Fig. 4. Typical diffuse modes in the phase transition, associated with frequency-dependent dielectric relaxation (i.e., gradually-decreasing maximum dielectric constants and increasing dielectric maximum temperatures, as the measurement frequency increased), are well demonstrated. Maximum dielectric constants and dielectric maximum temperatures of the BPZN system ($y = 0.08$) are 10,400 (56°C), 10,100 (61°C), 9,600 (68°C), and 9,000 (76°C) at 1 kHz, 10 kHz, 100 kHz, and 1 MHz, respectively, while those of the BPZT system ($y = 0.25$) are 695 (–123°C), 685 (–119°C), 675 (–107°C), and 660 (–93°C) at the same frequency decades.

Variations of the two dielectric parameters in the two systems are plotted in Fig. 5. As for the maximum dielectric constants, a peak value of 9,000 was observed at $y = 0.08$ in the BPZN system, whereas the value was only 660 at $y = 0.25$ in BPZT. The marked difference in the dielectric constant values between the BPZN and BPZT systems is believed to be attributed, at least in part, to the less active role of tantalum (which would favor the covalent bonds, as discussed previously) in the development of spontaneous polarization and also to the much higher threshold barium concentration in the BPZT system. Asymptotical decreases in the maximum dielectric constants with barium substitution in the two systems are also reported in $(\text{Ba}, \text{Pb})(\text{Mg}_{1/3}\text{Nb}_{2/3})\text{O}_3$ [20, 38], which can be accounted for by the gradual loss of long-range dipole interaction with replacements of Pb by Ba. Unlike the variations of the maximum dielectric constant, changes in the dielectric maximum temperatures were rather linear. However, the dielectric maximum temperatures in the BPZT system were much lower than those of BPZN, as is well reported [1, 30, 39]. Besides, the temperature

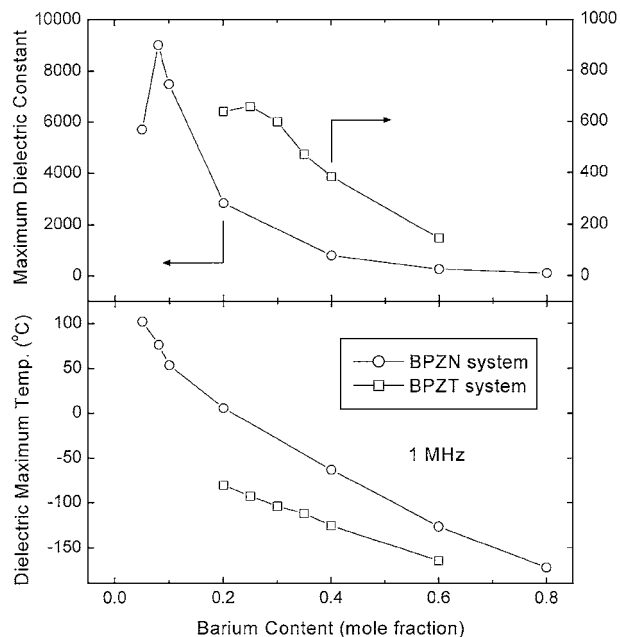


Figure 5 Dependencies of the maximum dielectric constant and dielectric maximum temperature upon composition.

difference between the two systems at the same barium content became gradually smaller from 86°C ($y = 0.2$) to 62°C ($y = 0.4$) and 36°C ($y = 0.6$).

4. Summary

Without any barium substitution, only a pyrochlore structure (along with negligible amounts of PbO and ZnO) was detected in the Pb-Zn-Nb-O and Pb-Zn-Ta-O mixtures of perovskite stoichiometries. In contrast, perovskite was the only structure developed at $0.08 \leq y$ and $0.35 \leq y$ in the BPZN and BPZT systems, respectively, i.e., threshold barium concentration (required for complete stabilization of the perovskite structure) is much smaller in the BPZN system than in BPZT. Meanwhile, pyrochlore and perovskite structures coexisted at intermediate compositions below the threshold barium concentrations. Comparative difficulty in the stabilization of the perovskite structure in the BPZT system was explained by the stronger covalency of Ta-O over Nb-O. Lattice parameters of the pyrochlore and perovskite structures increased with increasing amount of substituent barium in general, but changing rates in the perovskite were different below and above the threshold concentrations. Lattice parameters of the perovskite BZN and BZT were calculated to be 0.4094 and 0.4093 nm, while those of perovskite PZN and hypothetical PZT were extrapolated to be 0.4058 and 0.4050 nm, respectively. Highest values of the maximum dielectric constant in both systems were observed at compositions slightly below the threshold barium concentrations (i.e., 9,000 at $y = 0.08$ and 660 at $y = 0.25$ in the BPZN and BPZT systems), but the maximum value in the BPZN system is much higher than that in BPZT.

Acknowledgements

This study was supported by the Academic Research Fund for Advanced Materials (1997–1999) from the Ministry of Education, Republic of Korea.

References

1. V. A. BOKOV and I. E. MYL'NIKOVA, *Sov. Phys.-Solid State* **2** (1961) 2428.
2. Y. YOKOMIZO, T. TAKAHASHI and S. NOMURA, *J. Phys. Soc. Jpn.* **28** (1970) 1278.
3. Y. YOKOMIZO and S. NOMURA, *J. Phys. Soc. Jpn.* **28** (Suppl.) (1970) 150.
4. N. SETTER and L. E. CROSS, *J. Mater. Sci.* **15** (1980) 2478.
5. Y. MATSUO, H. SASAKI, S. HAYAKAWA, F. KANAMARU and M. KOIZUMI, *J. Amer. Ceram. Soc.* **52** (1969) 516.
6. J. WANG, D. WAN, J. XUE and W. B. NG, *ibid.* **82** (1999) 477.
7. S.-E. PARK, M. L. MULVIHILL, P. D. LOPATH, M. ZIPARRO and T. R. SHROUT, Proc. 10th IEEE ISAF, 1996, p. 79.
8. C. S. PARK, K. Y. LIM, D. Y. CHOI and S. J. CHUNG, *J. Kor. Phys. Soc.* **32** (Suppl.) (1998) S974.
9. T. R. SHROUT and A. HALLIYAL, *Amer. Ceram. Soc. Bull.* **66** (1987) 704.
10. S.-M. LIM and N.-K. KIM, *J. Mater. Sci.* **35** (2000) 4373.
11. M.-C. CHAE, S.-M. LIM and N.-K. KIM, *Ferroelectrics* **242** (2000) 25.
12. M. ONODA, J. KUWATA, K. KANETA, K. TOYAMA and S. NOMURA, *Jpn. J. Appl. Phys.* **21** (1982) 1707.
13. S. KAWASHIMA, M. NISHIDA, I. UEDA and H. OUCHI, *J. Amer. Ceram. Soc.* **66** (1983) 421.
14. S. B. DESU and H. M. O'BRYAN, *ibid.* **68** (1985) 546.
15. S. KAWASHIMA, *Amer. Ceram. Soc. Bull.* **72** (1993) 120.
16. F. GALASSO, L. KATZ and R. WARD, *J. Amer. Chem. Soc.* **81** (1959) 820.
17. A. I. AGRANOVSKAYA, *Bull. Acad. Sci. USSR, Phys. Ser.* **24** (1960) 1271.
18. F. GALASSO and J. PYLE, *Inorg. Chem.* **2** (1963) 482.
19. M. P. HARMER, J. CHEN, P. PENG, H. M. CHAN and D. M. SMYTH, *Ferroelectrics* **97** (1989) 263.
20. D. VIEHLAND, N. KIM, Z. XU and D. A. PAYNE, *J. Amer. Ceram. Soc.* **78** (1995) 2481.
21. H. TAMURA, D. A. SAGALA and K. WAKINO, *Jpn. J. Appl. Phys.* **25** (1986) 787.
22. R. D. SHANNON, *Acta Cryst. A* **32** (1976) 751.
23. J.-K. LEE, S.-G. KANG and H. KIM, *J. Mater. Sci.* **33** (1998) 693.
24. B.-Y. AHN and N.-K. KIM, *J. Amer. Ceram. Soc.* **83** (2000) 1720.
25. *Idem.*, *Mater. Res. Bull.* **35** (2000) 1677.
26. B.-H. LEE, N.-K. KIM, J.-J. KIM and S.-H. CHO, *Ferroelectrics* **211** (1998) 233.
27. B.-H. LEE and N.-K. KIM, *ibid.* **227** (1999) 87.
28. S. L. SWARTZ and T. R. SHROUT, *Mater. Res. Bull.* **17** (1982) 1245.
29. M.-C. CHAE, N.-K. KIM, J.-J. KIM and S.-H. CHO, *Ferroelectrics* **211** (1998) 25.
30. H. C. LING, M. F. YAN and W. W. RHODES, *ibid.* **89** (1989) 69.
31. *Idem.*, *J. Mater. Sci.* **24** (1989) 541.
32. W. F. SMITH, "Principles of Materials Science and Engineering," 2nd edn. (McGraw-Hill, 1990) p. 37.
33. T. MATSUOKA, S. KAWASHIMA, Y. MATSUO, S. HAYAKAWA, T. IKEDA, A. NAKAUE, K. INOUE and Y. YAGI, *J. Amer. Ceram. Soc.* **58** (1975) 321.
34. M.-C. CHAE and N.-K. KIM, *Ferroelectrics* **209** (1998) 603.
35. A. V. TITOV, O. I. CHECHERNIKOVA and YU. N. VENEVTSEV, *Inorg. Mater.* **14** (1978) 891.
36. S. NOMURA, K. KANETA and M. ABE, *Jpn. J. Appl. Phys.* **18** (1979) 681.
37. B.-H. LEE, N.-K. KIM, J.-J. KIM and S.-H. CHO, *J. Kor. Phys. Soc.* **32** (Suppl.) (1998) S978.
38. S. J. BUTCHER and N. W. THOMAS, *J. Phys. Chem. Solids* **52** (1991) 595.
39. V. J. JOHNSON, M. W. VALENTA, J. E. DOUGHERTY, R. M. DOUGLAS and J. E. MEADOWS, *ibid.* **24** (1963) 85.

Received 19 October 2000

and accepted 26 April 2002